HHS Public Access

Author manuscript

Magn Reson Med. Author manuscript; available in PMC 2016 May 01.

Published in final edited form as:

Magn Reson Med. 2015 May ; 73(5): 2025–2029. doi:10.1002/mrm.25309.

On conductivity, permittivity, apparent diffusion coefficient and their usefulness as cancer markers at MRI frequencies

Ileana Hancu, PhD[1], **Jeannette Christine Roberts, MS**[1], **Selaka Bulumulla, PhD**[1], and **Seung-Kyun Lee, PhD**[1]

[1]GE Global Research Center, Niskayuna, NY, USA

Abstract

Purpose—To investigate permittivity and conductivity of cancerous and normal tissues, their correlation to the apparent diffusion coefficient (ADC), and the specificity that they could add to cancer detection.

Methods—Breast adenocarcinomas and prostate carcinomas were induced in rats. Conductivity and permittivity measurements were performed in tumors and muscle tissue in the anesthetized animals, using a dielectric probe and an impedance analyzer, between 50 and 270MHz. The correlations between ADC's (measured at 3T) and probe-measured conductivity values were investigated. Frequency dependent discriminant functions were computed, to assess the value that each of the three parameters adds to cancer detection.

Results—27%/12%/7% permittivity contrast was observed between tumors and normal tissue at 64/128/270 MHz, respectively. Relatively frequency independent, 15–20% conductivity contrast was noted between cancerous and normal tissue. Strong negative correlation was observed between tissue conductivity and ADC. While permittivity had the strongest discriminatory power at 1.5T, it became comparable to ADC at 3T, and less important than ADC at 270 MHz.

Conclusion—Conductivity measurements offered limited advantages in separating cancer from normal tissue beyond what ADC already provided; conversely, permittivity added separation power when added to the discriminant function. The moderately high cancerous tissue permittivity and conductivity impose strong constraints on the capability of MRI-based tissue electrical property measurements.

Keywords

conductivity; permittivity; apparent diffusion coefficient; MRI; tumor; cancer

Introduction

Diffusion weighted imaging, and apparent diffusion coefficient (ADC) mapping are used increasingly frequently for cancer detection, alone or in addition to dynamic contrast enhanced MRI (1–3). While easy to acquire, ADC maps are usually not specific enough, and

Corresponding author: Ileana Hancu, GE Global Research Center, One Research Circle, K1-NMR133, Niskayuna, NY 12309, hancu@ge.com, tel: 518-387-4703, fax: 518-387-6923.

additional parameters are needed for tumor characterization. Recent demonstration of tissue electrical properties (TEP) mapping by MRI (4–6) has raised hopes that these parameters can increase the specificity of cancer detection. Unfortunately, TEP mapping is sensitive to noise, therefore prone to measurement error. Additionally, disagreements exist in the literature about the conductivity and permittivity of cancerous tissues; while some reports document less than 10% increases of electrical properties of cancerous tissues of cancers (7), others point to factors of 1.5, 2 or higher (8–10). It is therefore important to quantify the tumor/normal TEP differences by gold standard measurements, as a function of field strength, in order to establish the required capability for MRI based TEP measurements.

In addition, the suggested linear relationship between the conductivity and diffusion tensor eigenvalues (11) is also interesting to explore, to clarify the potential of TEP's as *independent* markers of disease. Using the observation that, although mediated by different carriers, both the conduction and the diffusion process respect the same boundary conditions imposed by the tissue geometry, Tuch et al. demonstrated that the conductivity and diffusion tensor share the same eigenvectors (11). A further, low frequency, approximation results in a linear relationship between the conductivity and diffusion tensor eigenvalues, enabling one to compute the conductivity out of the diffusion tensor (12). If conductivity and the apparent diffusion coefficient are linearly correlated, then measurement of the first one will add little or no information to tumor characterization-- in addition to what diffusion weighted imaging offers. Ultimately, the discriminatory power of each of these three parameters (permittivity, conductivity and ADC) for cancer detection needs to be understood, in order to guide further optimization of MRI based TEP mapping.

In this work, conductivity and permittivity measurements were performed in two rat tumor models using an impedance analyzer and a dielectric probe over the 50–270MHz range. Correlations between tumor conductivity and ADC's (measured at 3T) were also assessed. Discriminant functions that best separate benign from malignant tissues, using tissue conductivity, permittivity and ADC's as input, were constructed as a function of field strength. Recommendations regarding field strength and MRI based TEP mapping capability are offered in conclusion.

Methods

All the experiments described were done with approval of the Institutional Animal Care and Use Committee.

Tumor models and impedance analyzer based dielectric measurements

Cells from the MATBIII (breast adenocarcinoma) and MATLyLuB2 (prostate carcinoma) tumor lines were implanted in the flanks of 6 female Fisher (of 11 weeks mean age and 178g mean weight) and 7 male Copenhagen rats (of 11 weeks mean age and 256g mean weight). When tumors reached a spherical size of about 2cm diameter, imaging was performed, with the animals anesthetized using 1.5% Isoflurane, and their temperature maintained to 37C. Following the MRI scanning session, with rats still under anesthesia, the skin above the tumors was opened, and dielectric measurements over the 50–270MHz range were performed using an E4991 impedance analyzer and an E85070 dielectric probe (Agilent,

USA), pressed tightly against the tissue under study. The temperature of the animals was maintained by placing them on a heated pad between dielectric measurements. Due to the minute long duration of each measurement, lower room temperature, and low heat capacity of the dielectric probe, it is estimated that open tumor/muscle temperature varied by as much as 3°C from the nominal 37°C. The animals were sacrificed at the end of the session. Four to six measurements were taken in different places of the tumor and normal muscle, to increase measurement accuracy and compensate for the non-isotropic sensitivity of the dielectric probe in its intended sample volume of ~8cc. Note that, although it would have been preferable to extend the frequency range to 300MHz, in order to cover the common range of MRI frequencies, our instrument exhibited intermittent failure modes past 270 MHz. Given the relatively slow variation of the electrical properties over the range studied, we preferred to report all results at 270 MHz, instead of some results at 300MHz.

Imaging

All scans were done on a Discovery 3.0 T MR750 scanner (GE Healthcare, Waukesha, WI), using a transmit receive quadrature Litz coil (Doty Scientific, Columbia, SC), of 50mm diameter and 108mm length. Rats were placed on two tubes filled with warm solutions, with the tumors in the center of the coil. Following a localizer sequence, high resolution diffusion weighted images were acquired for 13 axial slices, at 1.5mm thickness, with a field of view 12×6cm, and x/y resolution of 0.9mm. For the first animal scanned, eleven b values, equally spaced between 0 and 1000 $*10^{-3}$ mm^2/s were acquired, to look for evidence of biexponential signal decay. Lacking this evidence, all other experiments were acquired with two b values (b_1=0 and b_2=600$*10^{-3}$ mm^2/s). ADC's were computed on a pixel by pixel basis, using $ADC=\ln(S[b_1]/S[b_2])/(b_2-b_1)$. Regions of interest (ROI's) were manually drawn on each diffusion weighted image, and average tumor ROI's were computed by averaging ADC's over each slice, and then over the 13 slices (which almost entirely covered the tumor).

Statistical analysis

SPSS 19 (IBM, Armonk, NY) was used for statistical data analysis. For each of the 13 animals studied, average conductivity and permittivity were computed from the dielectric measurements for tumor and muscle tissues at 64, 128 and 270MHz. Average muscle and ADC values, measured at 128MHz, were also used in the statistical analysis at 64 and 270MHz-- as they are frequency independent.

Pearson correlation coefficients between conductivity and ADC values were computed at the 3 frequencies studied. Stepwise discriminant analysis was also performed for each of the three frequencies, using the 26 average values (13 tumors and 13 muscle) of conductivity, permittivity and ADC, as input. Discriminant functions were computed at 64, 128 and 270MHz. To select predictors, Wilk's lambda method (which selects predictors that minimize Wilk's lambda) was employed. An F-statistic was used to threshold entering/exiting variables, so that only variables that add significant amount of orthogonal discriminatory power were selected in the discriminant function. The criteria for entry was an F-function probability of 0.05, and the criteria for removal was a F-function probability of 0.1.

Results

Figure 1 shows an overlay between the ADC image and the anatomical image, with the tumor region encircled by the green elliptical ROI; the dielectric probe placement (after the MRI exam) is also exemplified here in white. The two red circles in this image represent the warm solutions, of high ADC; as expected the tumors exhibit lower ADC than the surrounding, normal muscle tissue. Note that the size of the tumors we chose to investigate was dictated by the availability of commercial instrumentation for dielectric measurements; since such measurements are typically done on the basis of an S11 measurement from an open coaxial cable, all the fields emitted by the probe need to be contained within the sample. The relatively long wavelength characteristic of MRI frequencies dictates the minimum sample size in which measurements can be reliably done.

Figure 2 displays the tumor-muscle permittivity and conductivity differences (expressed in percent) for the MATBIII and MATLyLu tumors, as a function of frequency; the standard deviations reported are between animals. Since electrical properties are known to change with temperature by as much as 2%/°C (13), the percent change in electrical properties will depend on temperature only to a minimal extent- as the conductivity of both tissue types will be affected by the temperature changes in a similar manner. While some differences exist between the two tumor strains, the range of contrasts seen in the two cases are similar, varying, e.g., between 0 and 30% in conductivity and between 15 and 30% in permittivity at 64MHz. Decreasing permittivity contrast and somewhat constant conductivity contrast is seen progressing from 64, to 128 and to 270MHz. Note that higher variability is seen in the conductivity than in the permittivity measurements-- as error bars are considerably higher for the former. This fact is a direct reflection of the higher inter-subject (population) variability, as well as of the higher intra-subject conductivity measurement variability (8–10% for conductivity, vs. 2–5% for permittivity). High intra-subject variability in the conductivity measurements can be due to e.g., temperature sensitivity or inherent tumor heterogeneity. While the first can be mitigated by an *in vivo* measurement technique that does not expose tissue to colder room air (MRI, e.g.), the later is of a fundamental nature, and cannot be mitigated.

Figure 3 displays the correlation between ADC's and the probe-based conductivity measurements at 128MHz. In this graph, the dots represent experimental data points, the black line represents the linear fit, the red line the 95% confidence interval, and the blue line the 95% prediction interval. While higher ADC is associated with lower conductivity, the linear fit explains only a fraction of data variability (R^2=0.48). Pearson correlation coefficients between ADC and conductivity values at the 3 frequencies are all around −0.65, and the correlation is significant at the 0.001 level (two-tailed).

Following stepwise discriminant analysis at the 3 frequencies, Table 1 shows the standardized canonical discrimination function coefficients and Wilk's lambda (defining the proportion of the total variance in the discriminant scores not explained by differences among the groups). As coefficients with large absolute values correspond to variables with greater discriminating ability, the field strength dependence of TEP's imparts a strong weight on the capability of different factors to discriminate between cancer and normal

tissue. While permittivity has the strongest discrimination power at 1.5T, it becomes comparable to ADC at 3T, and less important than ADC at 7T. Conversely, conductivity measurements impart limited or no incremental discrimination power above ADC; note that even at 128MHz, if only ADC and conductivity are entered as independent variables in the discriminant analysis, only ADC ends up part of the discriminant function. Whether this is due to the ADC correlation to conductivity, or to the high intra-subject or inter-subject variability remains to be determined.

Discussion and Conclusions

This study offers insight into the electrical properties of tumors, and their potential usefulness as cancer markers at MRI frequencies. Somewhat limited differences between electrical properties of the two tumors lines studied here and normal muscle tissues were found, averaging 26% in permittivity and 14% in conductivity at 64MHz. The permittivity differences consistently decreased as frequency increased, reaching 7% at 270MHz, while conductivity differences remained relatively constant across the 50–270MHz range studied here. Our results are consistent with a number of literature studies (9,13), yet not so consistent with others (7,14). While some of the discrepancies between our data and similar published reports can be explained by the exact type of tumor studied, measurement technique and protocols can also undesirably influence results. For example, in our in-situ, dielectric probe based measurements, we see smaller tumor conductivity values than measured in breast cancer patients through MRI-based approaches (14). In fact, the highest conductivity of any tumor measured by us at 128MHz is 0.89S/m--significantly below the 1.5–6S/m reported elsewhere (14). Given the small size of the tumors previously studied (14), the known susceptibility of MRI-based methods to region of interest edge effects, and the relatively well-understood mechanisms determining electrical properties (which limit TEP's to the properties of extracellular fluid, i.e. conductivity of ~1.8S/m and relative permittivity of ~80 @128MHz) (13), is it is possible that MRI based methods could bias results (particularly for small ROI's), and their output needs to be regarded with caution. In our study, we also saw larger tumor/normal muscle electrical property differences than the less than 10% changes reported in a large scale study of breast tissue specimens, analyzed 0–4hrs after surgery (7). While following three of our animals after death, and taking repeated measurements every 30min, up to two hours after death (while maintaining the animals' core body temperature to 37°C), we have found slight changes in the electrical properties of both muscle and tumor tissue (data not shown). Electrical properties of tumors tended to decrease after death, and electrical properties of muscle tended to increase, resulting in an average contrast decrease after death from 30% to 22% in permittivity, and from 12% to 3% in conductivity (@ 64MHz). For the numbers reported here after death, electrical properties measured at 30, 60, 90 and 120min after death were averaged. While these changes are not dramatic, they point to the need to reference measurements taken by any imaging method to gold standard measurements also acquired *in vivo*-- if at all possible.

The negative correlation between tissue conductivity and ADC's at RF frequencies was somewhat expected, given prior work documenting low ADC and high conductivity for tumor tissues (1,14). While low frequency, theoretical and experimental studies find a positive correlation between the diffusion and conductivity eigenvalues (11,12,15), limited

theoretical work relating the diffusion and conductivity tensor eigenvalues exists in the high frequency regime. Given the results of a simulation study modeling a cell in uniform and heterogeneous electrical fields (16), and extensive studies analyzing the dielectric dispersion in tissues (13), the 64–300MHz regime characteristic of MRI experiments resembles the high frequency regime (in which cell membranes do not offer a significant barrier to current flow) much more than the low frequency regime. Our experimental results, indicating a negative correlation between conductivity and ADC remain to be explained by a theoretical model.

Discriminant analysis indicated that permittivity could add significant power in separating cancer from normal tissue, above and beyond what ADC offers. In fact, at 64MHz, permittivity accounted for a larger fraction of data variability than ADC's did (Table 1). As the field strength increased, and the difference between normal and malignant tissue permittivity decreased, permittivity added less and less differentiation power. Conductivity contributed little to increasing cancer characterization above what ADC did- at any frequency. These results are only valid assuming that electrical property measurement precision/accuracy is comparable to the one of this study. Should permittivity measurements be made by other means than dielectric probe (from MRI measurements, e.g.), and should measurement accuracy decrease from the current 2–5% to more than 10%, it is likely that such measurements would contribute less and less to cancer characterization, in particular at high field strengths, where permittivity differences dwindle. Conversely, should the accuracy of conductivity measurement improve from the 8–10% of the current study (by performing such measurements through imaging, and eliminating the slight temperature variation during the experiments, e.g.), it is possible for conductivity measurements to add value in the quest towards better cancer detection. Since the capability to estimate TEP's by MRI methods increases at higher field strengths (17), more accurate conductivity mapping at fields higher than 3T may provide the right direction. On the other hand, alternative methodology for reliable permittivity measurements at frequencies below 64MHz may also be useful.

Acknowledgments

This work was supported by the Grant R01CA154433 from the National Cancer Institute.

References

1. Partridge SC, DeMartini WB, Kurland BF, Eby PR, White SW, Lehman CD. Quantitative diffusion-weighted imaging as an adjunct to conventional breast MRI for improved positive predictive value. AJR Am J Roentgenol. 2009; 193(6):1716–1722. [PubMed: 19933670]
2. Kim SH, Cha ES, Kim HS, Kang BJ, Choi JJ, Jung JH, Park YG, Suh YJ. Diffusion-weighted imaging of breast cancer: correlation of the apparent diffusion coefficient value with prognostic factors. J Magn Reson Imaging. 2009; 30(3):615–620. [PubMed: 19711411]
3. Matsuoka A, Minato M, Harada M, Kubo H, Bandou Y, Tangoku A, Nakano K, Nishitani H. Comparison of 3.0-and 1. 5-tesla diffusion-weighted imaging in the visibility of breast cancer. Radiat Med. 2008; 26(1):15–20. [PubMed: 18236129]
4. Bulumulla SB, Lee SK, Yeo DT. Conductivity and permittivity imaging at 3.0T. Concepts Magn Reson Part B Magn Reson Eng. 41B(1):13–21. [PubMed: 23599691]

5. Katscher U, Voigt T, Findeklee C, Vernickel P, Nehrke K, Dossel O. Determination of electric conductivity and local SAR via B1 mapping. IEEE Trans Med Imaging. 2009; 28(9):1365–1374. [PubMed: 19369153]

6. Wiesinger, F. Prospects of Absolute B1 Calibration. Seattle, WA: 2006.

7. Lazebnik M, et al. A large-scale study of the ultrawideband microwave dielectric properties of normal, benign and malignant breast tissues obtained from cancer surgeries. Phys Med Biol. 2007; 52(20):6093. [PubMed: 17921574]

8. Gabriel S, et al. The dielectric properties of biological tissues: III. Parametric models for the dielectric spectrum of tissues. Phys Med Biol. 1996; 41(11):2271. [PubMed: 8938026]

9. Joines WT, Zhang Y, Li C, Jirtle RL. The measured electrical properties of normal and malignant human tissues from 50 to 900 MHz. Med Phys. 1994; 21(4):547–550. [PubMed: 8058021]

10. Surowiec AJ, Stuchly SS, Barr JB, Swarup A. Dielectric properties of breast carcinoma and the surrounding tissues. IEEE Trans Biomed Eng. 1988; 35(4):257–263. [PubMed: 2834285]

11. Tuch DS, Wedeen VJ, Dale AM, George JS, Belliveau JW. Conductivity tensor mapping of the human brain using diffusion tensor MRI. Proc Natl Acad Sci U S A. 2001; 98(20):11697–11701. [PubMed: 11573005]

12. Haueisen J, Tuch DS, Ramon C, Schimpf PH, Wedeen VJ, George JS, Belliveau JW. The influence of brain tissue anisotropy on human EEG and MEG. Neuroimage. 2002; 15(1):159–166. [PubMed: 11771984]

13. Foster KR, Schwan HP. Dielectric properties of tissues and biological materials: a critical review. Crit Rev Biomed Eng. 1989; 17(1):25–104. [PubMed: 2651001]

14. Katscher U, Abe H, Ivancevic M, Djamshidi K, Karkowski P, Newstead G. Towards the investigation of breast tumor malignancy via electric conductivity measurement. 2013:3372.

15. Sotak CH. Nuclear magnetic resonance (NMR) measurement of the apparent diffusion coefficient (ADC) of tissue water and its relationship to cell volume changes in pathological states. Neurochem Int. 2004; 45(4):569–582. [PubMed: 15186924]

16. Gowrishankar TR, Stewart DA, Weaver JC. Model of a confined spherical cell in uniform and heterogeneous applied electric fields. Bioelectrochemistry. 2006; 68(2):181–190. [PubMed: 16230052]

17. van Lier AL, Raaijmakers A, Voigt T, Lagendijk JJ, Luijten PR, Katscher U, van den Berg CA. Electrical Properties Tomography in the Human Brain at 1.5, 3, and 7T: A Comparison Study. Magn Reson Med.

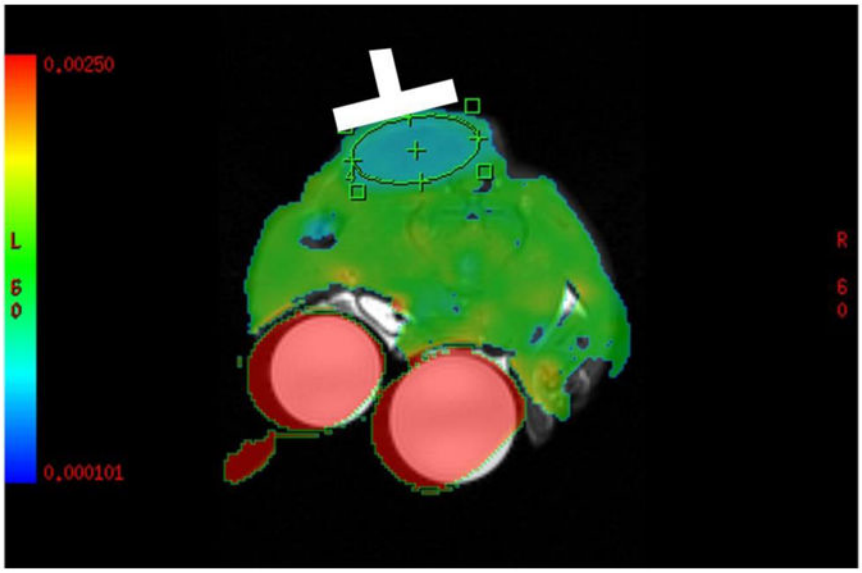

Figure 1.
Example of the overlay between the ADC map and the anatomical image. Dielectric probe placement, following the imaging experiment, is highlighted here in white

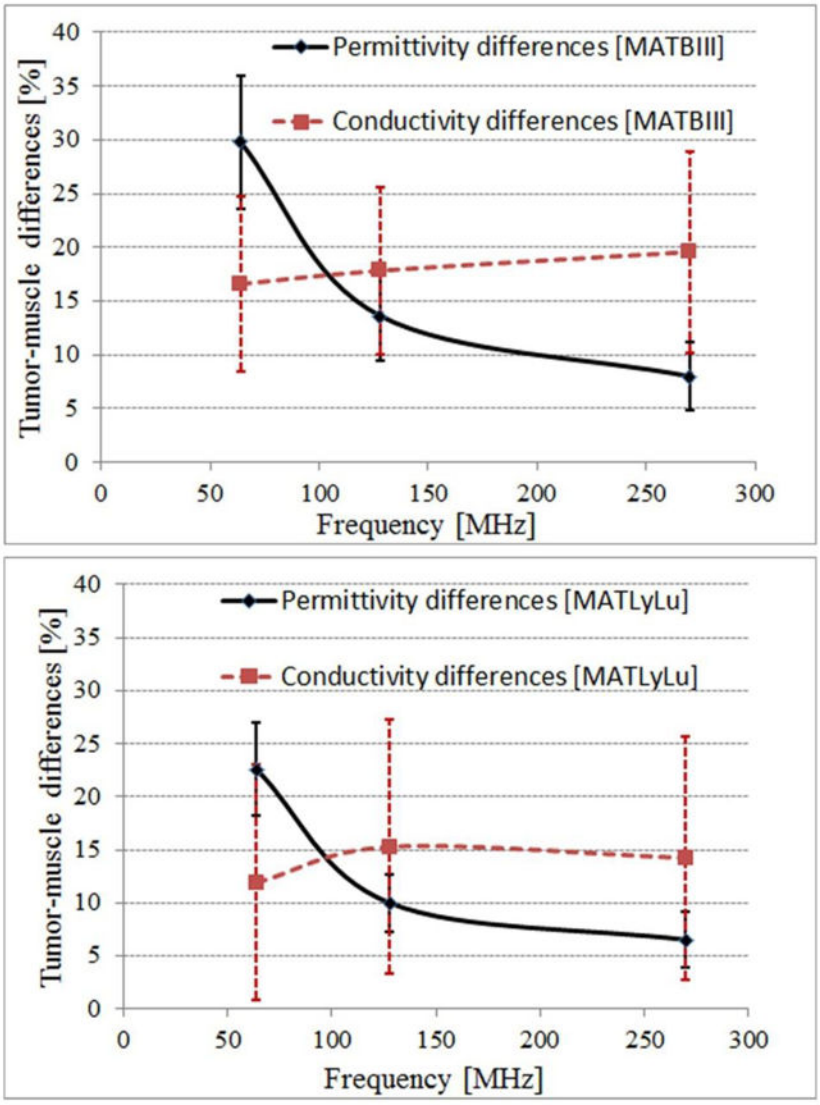

Figure 2.
Tumor-muscle TEP differences for the MATBIII (top) and MATLyLu (bottom) strains as a function of frequency.

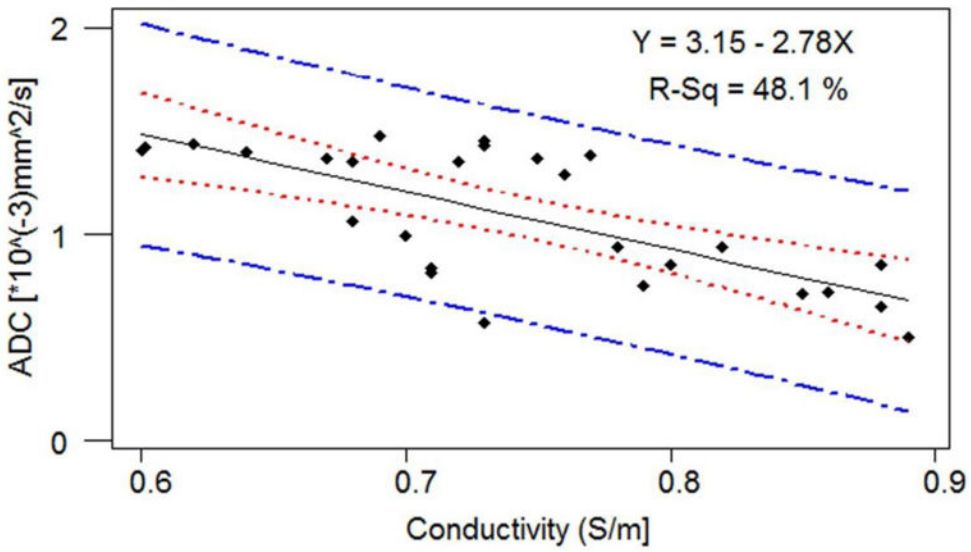

Figure 3.
Correlation between ADC and conductivity at 128MHz.

Table 1

Standardized canonical discrimination function coefficients. Wilk's lambdas are displayed in parentheses, for each variable separately, and for the combined discriminant function (under the Frequency column)

Frequency [MHz]	ADC	Permittivity	Conductivity
64 (0.04)	−0.7 (0.15)	0.9 (0.07)	0 (0.6)
128 (0.06)	−1 (0.15)	1 (0.19)	0.6 (0.6)
270 (0.09)	0.9 (0.15)	−0.7 (0.35)	0 (0.6)